THE ASIAN BULLETIN OF BIG DATA MANAGMENT
Vol. 5. Issue 4 (2025)
https://doi.org/10.62019/xbfpq253

ASIAN BULLETIN OF BIG DATA MANAGEMENT
http://abbdm.com/
ISSN (Print): 2959-0795
ISSN (online): 2959-0809

# Flavone Hydrazide Thiourea Derivatives: Synthesis, anti-diabetic, and in silico QSAR Analysis

Javeria Shaikh, Waqas Jamil, Samreen Zainalabdin

**Chronicle**

**Article history**
**Received**: Sept 2, 2025
**Received in the revised format:** Oct 5, 2025
**Accepted:** Oct 23 2025
**Available online:** Nov 28, 2025

**Javeria Shaikh,** are currently affiliated with the Dr. M.A. Kazi Institute of Chemistry, University of Sindh, Jamshoro, Pakistan.

**Email:** javeriashaikh2116@gmail.com

**Waqas Jamil,** are currently affiliated with the Dr. M.A. Kazi Institute of Chemistry, University of Sindh, Jamshoro.

**Email:** waqas.jamil@usindh.edu.pk

**Samreen Zainalabdin,** are currently affiliated with HEJ Karachi University Pakistan.

**Email:** Samreenzain302@gmail.com

**Corresponding Author***

**Abstract**

This study reports synthesis of Flavone Hydrazide Thiourea Derivatives 2-21 with diverse functionalities for the cure of diabetic mellitus and their α-glucosidase inhibitor and in silico (computational) studies. In this regard, Flavone derivatives 2-21 has synthesized according to scheme and characterized by various spectroscopic techniques. These compounds showed significant potential towards α-glucosidase enzyme inhibition activity and found to be many fold better active than the standard Acarbose (IC50 =39.45±0.11µM). The IC50 values ranges 1.09-38.1µM. Among these, Compound 2 (IC50 = 3.16 ±0.29 µM) and 3 (IC50 = 2.12 ±0.78 µM) showed marvelous inhibition activity. Both these derivatives have –OH substitution at ring D. The molecular docking analysis revealed that these molecules have high potential to interact with the protein molecule and have high ability to bind with the enzyme. Furthermore, the computational study regarding drug likeness of molecules were also performed. The physicochemical and pharmacokinetics study showed that these compounds have excellent parameters required for drug likeness. The derivatives have high ability by GI absorption.

**Keywords:** Green banking activities, sustainable financing, corporate reputation, environmental performance.



## INTRODUCTION

Diabetes mellitus (DM) is a worldwide condition that threatens public health (Chen et al., 2012). Diabetes is on the rise, and the World Health Organization predicts that by 2030, it will be the sixth leading cause of death globally. (Chen et al., 2012)(World Health Organization & International Diabetes Federation, n.d.). It is a metabolic disorder in which blood glucose levels rise due to defects in insulin action, synthesis, or both (insulin is insufficient or inefficient)(Akkati et al., 2011). According to the International Diabetes Federation, it affected around 415 million people aged 20 to 79 in 2015. Another 200 million people are expected to be affected by diabetes by 2040, making it a global public health issue.(Zheng et al., 2018). Type-1, Type-2, and gestational diabetes are the three forms of diabetes based on a etiology and clinical presentation (GDM) (Malek et al., 2019). Type-I Diabetes Mellitus (T1DM) is defined by the autoimmune death of insulin-producing beta cells in the pancreas and accounts for 5% to 10% of all diabetes cases (Choi & Chung, 2016) (Maahs et al., 2010) (Daneman, 2006). It is primarily caused by an autoimmune destruction of pancreatic cells by a T-cell mediated inflammatory response (insulitis) and a humoral (B cell) reaction (Devendra et al., n.d.). As a result, there is a severe scarcity of insulin. Autoimmunity has been related to a combination of genetic susceptibility and environmental factors such as viral infection, toxins, and nutritional factors. Type 1 diabetes accounts for 80%-90% of childhood and adolescent diabetes (Craig et al.,

2009). T1DM is most common in adolescents and teenagers, but it can affect anyone at any age. More than 90%-95% of diabetes patients belong to Type-II Diabetes Mellitus (T2DM) and most of these patients are adults (Dabelea et al., 2014). Insulin resistance is defined as a decreased response to insulin in persons with T2DM. In this state, insulin is in efficient, hence an increase in insulin production is utilized to maintain glucose homeostasis. However, insulin synthesis declines over time, eventually leading to T2DM. T2DM is most common in people over the age of 45. Despite this, it is becoming increasingly common in children, teenagers, and younger people because to increased levels of obesity, physical inactivity, and energy-dense diets (Picke et al., 2019).

Miglitol, Voglibose, Acarbose and Nojirimycin are glycosidic base *a*-glucosidase inhibitors that are being utilized to manage glucose levels in diabetes patients. These inhibitors despite their potency have several draw back, including diarrhea, stomach distention, meterorism and flatulence. Due to various side effects and absorptivity issues with existing inhibitors, it is need of time to develop more influential and safer *a*-glucosidase inhibitors (Proença et al., 2017).

## MATERIALS AND METHODS

All Nuclear Magnetic Resonance (NMR) experiments had been carried out using on Advance Bruker 300 MHz. Elemental analysis and Electron impact mass spectra (EI-MS) was performed on Finnigan MAT-311A, Germany, Elemental Analysis (CHN/S) on Elemental Perkin Elmer 2400-II Analyzer, United States respectively.

### Synthesis of Flavone Hydrazide

The key intermediate 4-(6-hydroxy-4-oxo-4H-benzopyran-2- yl)-benzoic acid hydrazide (Flavone hydrazide) 1 was synthesized in four (4)-steps. Step-1 is synthesis of chalcone. Step-2 the cyclization of chalcone. Step-3 is synthesis of flavone methyl ester. Step-4 is synthesis of flavone hydrazide.

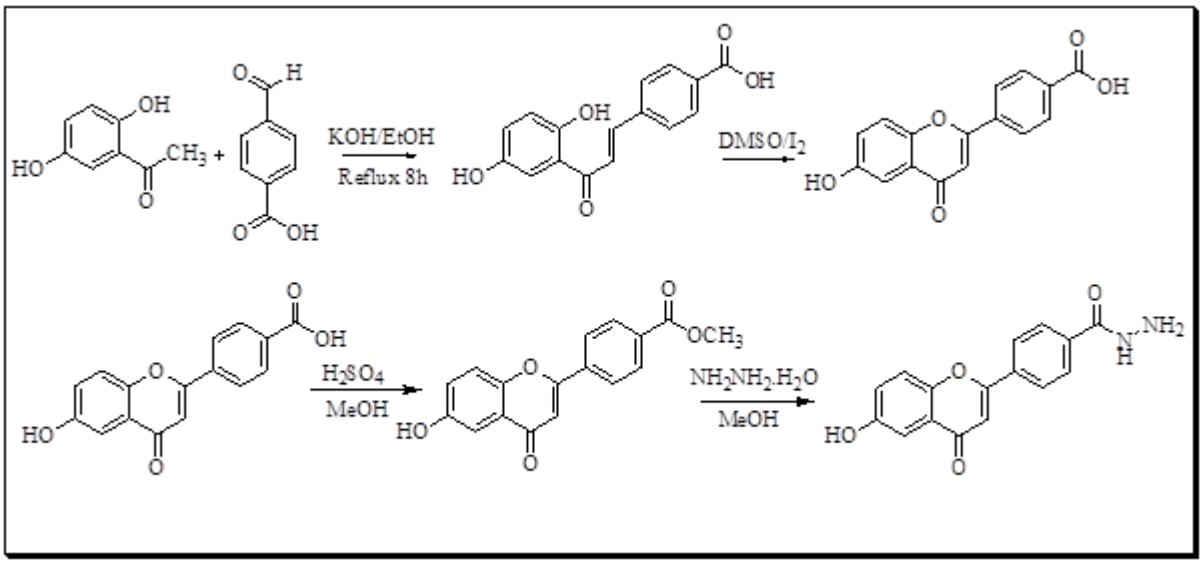


**Figure1.**
**Synthesis of Flavone Hydrazide**

### Synthesis of Flavone Hydrazide Thiourea Derivatives 2-21

Synthesis of flavone hydrazide thiourea derivatives **2-21** were synthesized by treating flavone hydrazide with various aryl isothiocyanates in THF. The mixture was stirred for

16 h at room temperature. After 16 h the solvent was evaporated and various colored precipitates were obtained. The precipitates were washed with ethanol and dist. water for the removal of any unreacted material. Finally, the products were recrystallized with ethanol in order to get pure compound **2-21**.

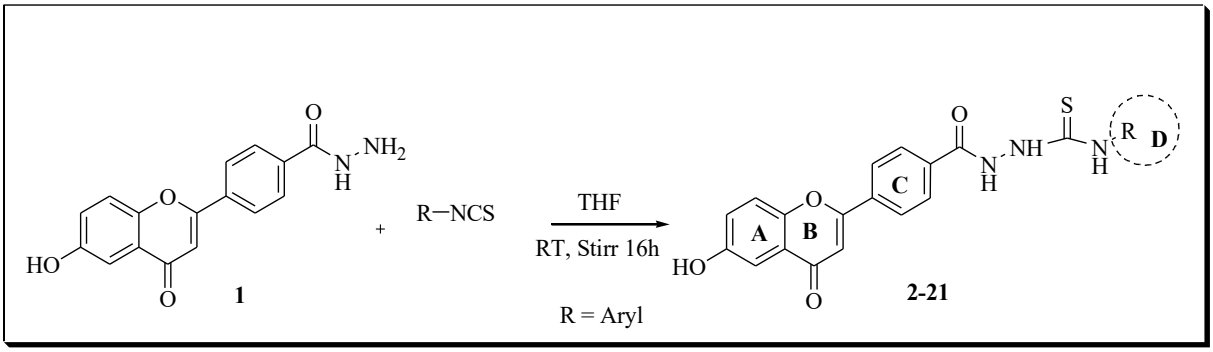


**Figure 2.**
**Synthesis of Flavone Hydrazide Thiourea Derivatives 2-21**

**Table 1.**
**R Group Representation**

| S.No | R | S.No | R | S.No | R |
|---|---|---|---|---|---|
| 2 | 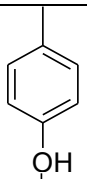 | 9 | 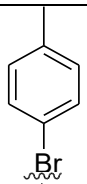 | 16 | 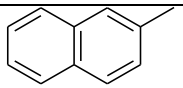 |
| 3 | 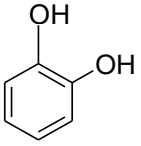 | 10 | 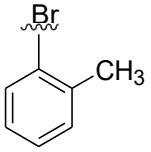 | 17 | 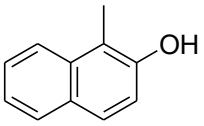 |
| 4 | 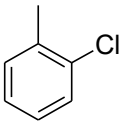 | 11 | 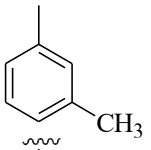 | 18 | 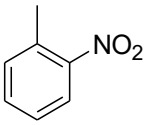 |
| 5 | 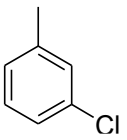 | 12 | 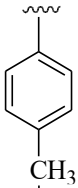 | 19 | 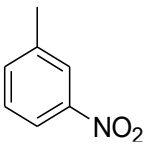 |
| 6 | 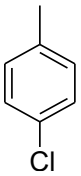 | 13 | 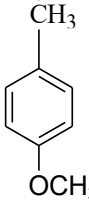 | 20 | 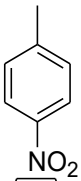 |
| 7 | 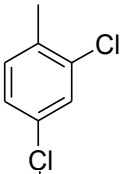 | 14 | 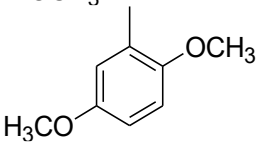 | 21 | 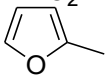 |
| 8 | 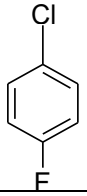 | 15 | 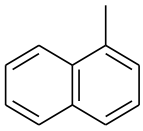 | | |

***α*-Glucosidase Inhibition Activity**

**Table 2.**
***α*-Glucosidase Inhibition Activity**

| S.# | $IC_{50}$ μM ± SEM[a] | S.# | $IC_{50}$ μM ± SEM[a] |
|---|---|---|---|
| **2** | 3.16 0.29 | **12** | 22.78 ± 0.65 |
| **3** | 2.12 0.78 | **13** | 29.63 ± 0.44 |
| **4** | 7.19±0.45 | **14** | 33.57±0.78 |
| **5** | 8.33 ±0.97 | **15** | 41.16 ± 1.22 |
| **6** | 6.23 ±1.11 | **16** | 40.58 ± 1.46 |
| **7** | 7.46±0.54 | **17** | 15.34 ± 1.66 |
| **8** | 5.44±1.23 | **18** | 45.56 ± 0.87 |
| **9** | 11.68±1.52 | **19** | 50.39 ± 0.1.12 |
| **10** | 28.11±0.24 | **20** | 43.67 ± 1.23 |
| **11** | 25.31±0.98 | **21** | 33.12 ± 1.45 |
| **Acarbose (Standard)** | | | **39.45 ± 0.11** |

Compound **2** ($IC_{50}$ = 3.16 ±0.29 μM) and **3** ($IC_{50}$ = 2.12 ±0.78 μM**)** showed marvelous inhibition activity. Both these derivatives have –OH substitution at ring **D.** The higher activity may be due to high number of interaction site available with the enzyme.

Among halogens substituted compounds **4-9,** floro substituted compound **8** ($IC_{50}$ = 5.44 ±1.23 μM), chloro substituted compounds **4** ($IC_{50}$ = 7.19 ±0.45 μM), **5** ($IC_{50}$ = 8.33 ±0.97 μM), **6** ($IC_{50}$ = 6.23 ±1.11 μM), **7** ($IC_{50}$ = 7.46 ±0.54 μM) and bromo substituted compound **9** ($IC_{50}$ = 11.68 ±1.52 μM) also shown excellent activity. According to $IC_{50}$ values the floro substituted derivatives was found to be most active among them.

The $–CH_3$ and $-OCH_3$ groups substituted compounds **10** ($IC_{50}$ = 28.11±0.24), **11** ($IC_{50}$ = 25.31±0.98 μM), **12** ($IC_{50}$ = 22.78 ±0.65 μM), **13** ($IC_{50}$ = 29.63 ±0.44 μM), and **14** ($IC_{50}$ = 33.57 ±0.78 μM) was also found to be better active than the standard although their activity was found to be less than the compounds having –OH or halogen substituted compounds.

Among napthalene ring containing derivatives **15** ($IC_{50}$ = 41.16 ±1.22 μM), **16** ($IC_{50}$ = 40.58 ±1.46 μM), and **17** ($IC_{50}$ = 15.34 ±1.66 μM), only compound **17** showed higher activity than the standard it is might be due to an –OH substitution on napthalene ring. The heterocyclic ring containing derivative **21** ($IC_{50}$ = 33.12 ±1.45 μM) also found be better active than the standard.

The $-NO_2$ substituted derivatives **18** ($IC_{50}$ = 45.56 ±0.87 μM), **19** ($IC_{50}$ = 50.39 ±1.12 μM), **20** ($IC_{50}$ = 43.67 ±1.23 μM) showed moderate inhibition activity. The decline in activity might be due to some electron withdrawing effect of $–NO_2$ group.

The heterocyclic ring containing derivative **21** ($IC_{50}$ = 33.12 ±1.45 μM) also found be better active than the standard. For better understanding of structure–activity relationship these compounds were subjected to computational studies.

For better understanding of structure–activity relationship these compounds were subjected to computational studies.

# COMPUTATIONAL ANALYSIS

## Homology Modeling of *α* -Glucosidase Enzyme

With the aid of the homology modeling technique, the 3D structure of the enzyme *α*-glucosidase from Saccharomyces cerevisiae (Baker's yeast) was developed. (PDB ID: 3A4A; Supporting Information) [**36**] (Yousuf et al., 2018).

## Molecular Docking Analysis

Using the software Patchdock server, molecular docking studies of biologically active compounds against the targeted receptor were carried out to observe the binding pattern of potent *a*-glucosidase inhibitors.

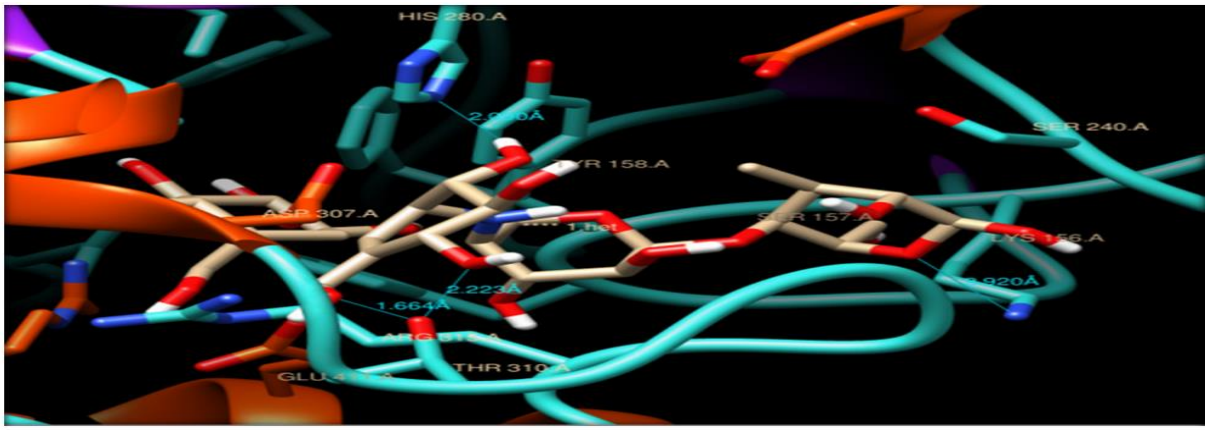


**Figure 4.**
**Molecular docking of drug Acarbose showing interactions with a.a residues Lys 156, His 280 and Arg 315 within the binding pocket of 5 Å region.**

Compound **2** is found to be the most potent inhibitor of series with ($IC_{50}$ = 2.12 ±0.78 *μ*M) almost 37 times more potent inhibitor comparative to standard drug acarbose ($IC_{50}$ = 39.45 ±0.11 *μ*M), The dock pose analysis of the compound is showing one H-bonding of amide oxygen atom with active site a.a residue LYS156, another H-bonding is observed b/w NH and Leu 313.however His 280 is also present within the provided 5A° region, while pi-pi stacking interactions are also possible **Fig.5**

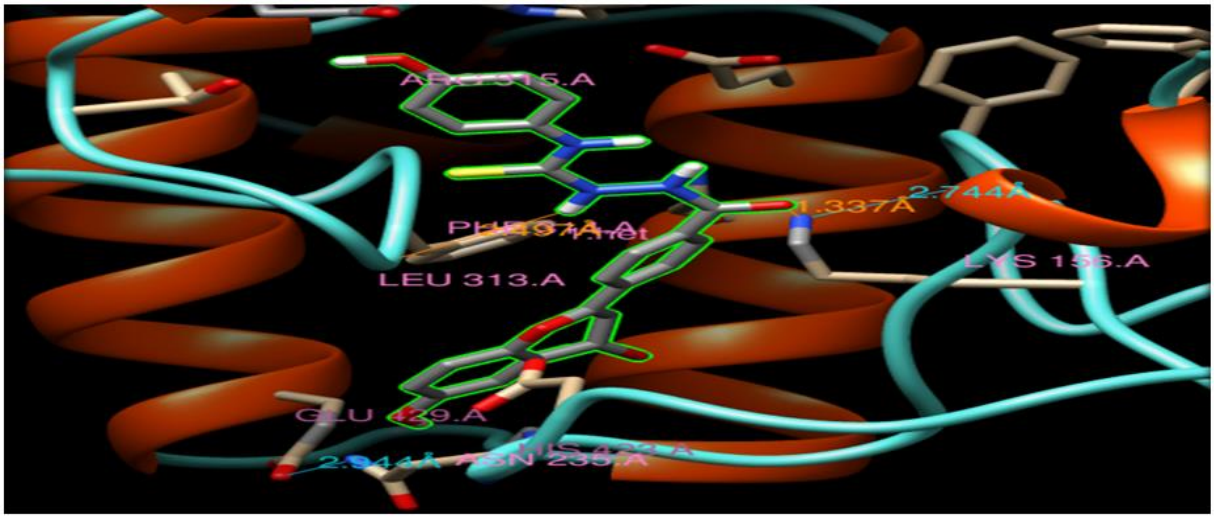


**Figure 5.**
**Dock pose of Compound 2**

Compound **1** is found to be the second most potent inhibitors of series with ($IC_{50}$=, 3.16 ±0.29 *μ*M**)** comparative to standard drug acarbose ($IC_{50}$ = 39.45 ±0.11 *μ*M). The dock pose analysis of the compound is showing one H-bonding of 6-hydroxy with active site a.a residue His 280, while another H-bonding is also observed b/w chrome oxygen and Gln 285, while active site a.a Lys 156 is also present within 5 A° region **Figure 6**.

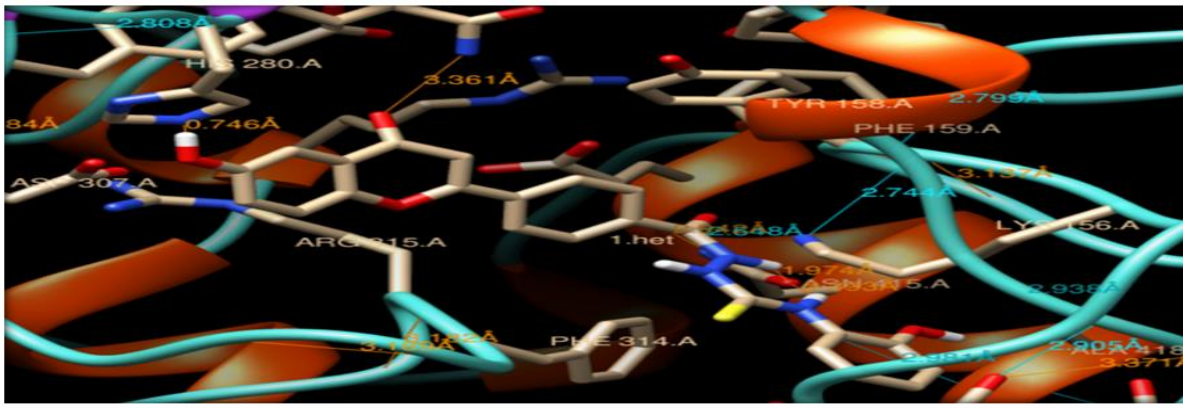


**Figure 6.**
**Dock pose of Compound 2**

Compound **7** is found to be the third most potent inhibitors of series with ($IC_{50}$ = 5.44 ±1.23 *μ*M) comparative to standard drug acarbose ($IC_{50}$ = 39.45 ±0.11 *μ*M**)**. The dock pose analysis of the compound is showing one H-bonding of 6-hydroxy with active site a.a residue His 280, while another H-bonding is also observed b/w NH and Lys 156 of active site a.a residue however chrome oxygen is making H-bond with Gln 285 **Fig.7**.

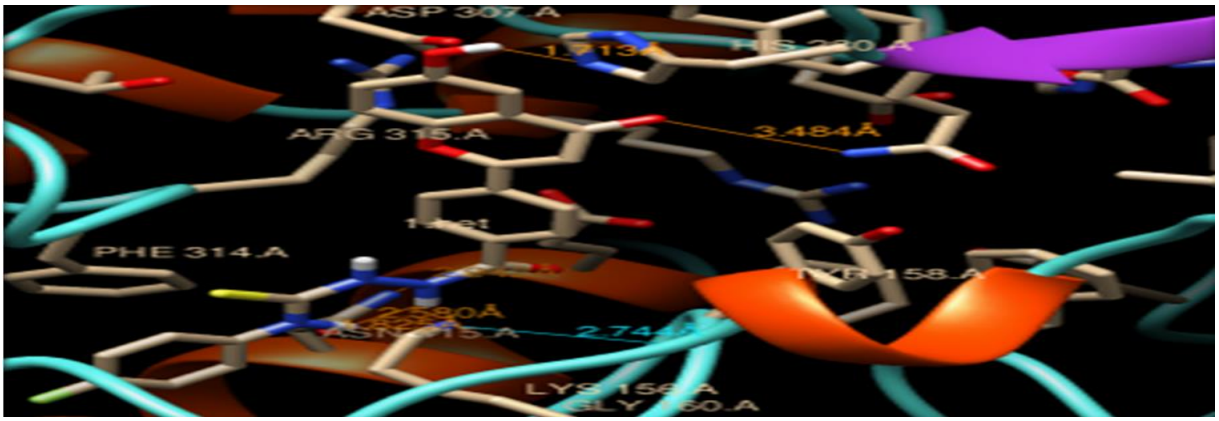


**Figure 7.**
**Dock pose of Compound 8**

Compound **6** is found to be the fourth most potent inhibitor of series with ($IC_{50}$ = 6.23 ±1.11*μ*M) comparative to standard drug acarbose ($IC_{50}$ = 39.45 ±0.11 *μ*M). The dock pose analysis of the compound is showing one H-bonding of 6-hydroxy with active site a.a residue His Asn 235, while another H-bonding is also observed b/w NH and Lys 156 of active site a.a residue however S is making H-bond with Tyr 316 **Fig.8**.

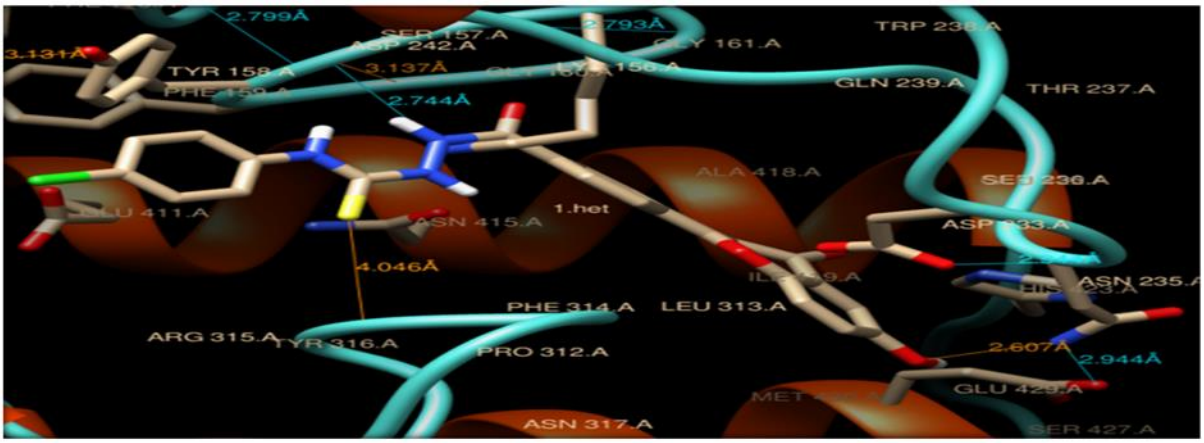

**Figure 8.**
**Dock pose of Compound 6**

Compound **4** is found to be the fifth most potent inhibitor of series with ($IC_{50}$ = 7.19 ±0.45*μ*M) comparative to standard drug acarbose ($IC_{50}$ = 39.45 ±0.11 *μ*M). The dock pose analysis of the compound is showing one H-bonding of amide carbonyl oxygen with active site a.a residue within the provided 5A° region.

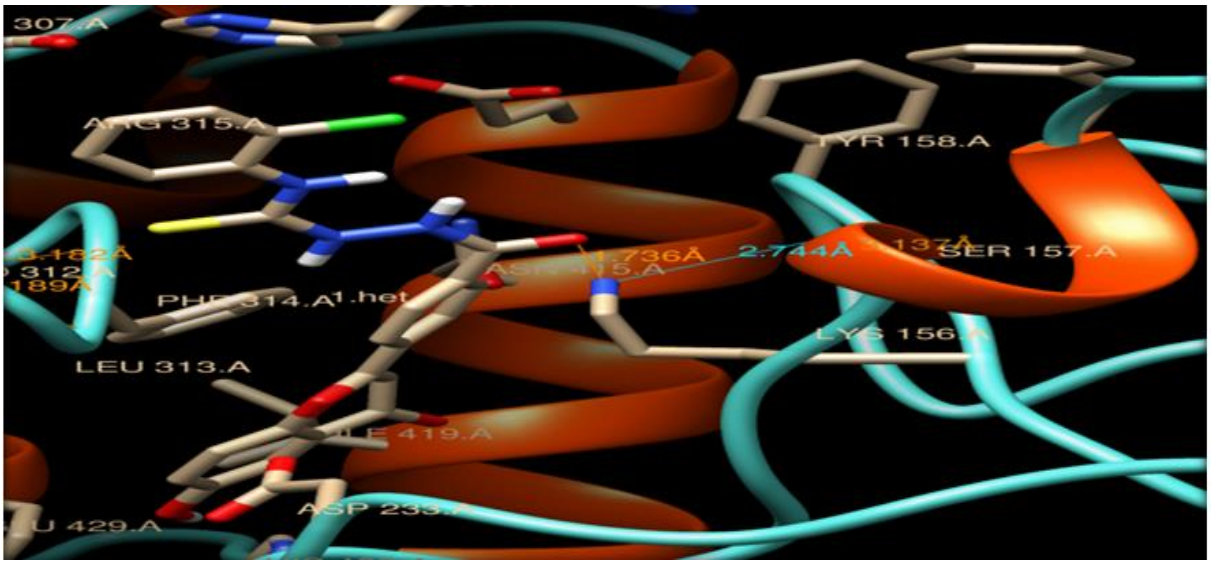


**Figure9.**
**Dock pose of Compound**

## Profiling of Pharmacokinetics Properties of Potent *α* -Glucosidase Inhibitors

*α* -Glucosidase inhibitors were also profiled against p-gp (Permeability of glycoproptein) and isozymes of CYP450 through Swiss ADME tools (Daina & Zoete, 2016), to predicts which compound can be inhibitor of p-gp, and against different CytochromeP450 (CYP450) isozymes. PGlycoprotein is an important protein in pharmaceutical research due to its substantial effect on ADME (Absorption, Distribution, Metabolism and Excretion) properties. In our screen compounds **2–21** exhibited high GI absorption, only three compounds **10,11,12** showed Blood Brain Barrier (BBB) permeability and none of compounds showed Pgp substrate and however, compounds **4,5,6,8-13** and **15** are predicted to be the CYP1A2 isozyme inhibitors. All the compounds showed inhibition except **16,18** against CYP2C19. None of the compound showed inhibition against CYP2D6 while compounds **4,5,6,10-14,19-21** showed inhibition against CYP3A4 respectively, therefore, they can show Drug–Drug Interactions (DDI)

## Physicochemical Properties Profiling of Potent *α* -Glucosidase Inhibitors

According to the Lipinski rule there are various physicochemical descriptors to describe the properties of molecules (Lipinski et al., 1997), including molecular weight, numbers of hydrogen bond donor (HBD), number of hydrogen bond accepter (HBA), the octanol/water partition coefficient (log P) should be 500, 5, 10 and 5, respectively, while the Total Polar Surface Area (TPSA) due to nitrogen (N) and sulfur (S) atoms should be in the range 20–130 A2 . In our case of study all the screened compounds successfully filtered and showed excellent drug ability properties according to Rule of Five (ROF), however, compounds **8** and **9** exceeds WLOGP very slightly greater than 5, while compounds **2**, **3** and **16–19** also slightly exceeds the TPSA greater than 130 A All the compounds are showing excellent drug ability properties according to ROF.

**Table3.**

**Pharmacokinetics Properties of Potent *a* -Glucosidase Inhibitors**

| Comp# | GI absorption | BBB absorption | Pgp substrate | CYP1A2 Inhibitor | CYP2C19 Inhibitor | CYP2C9 inhibitor | CYP2D6 inhibitor | CYP3A4 Inhibitor |
|---|---|---|---|---|---|---|---|---|
| **2** | High | No | No | No | Yes | Yes | No | No |
| **3** | High | No | No | No | Yes | Yes | No | No |
| **4** | High | No | No | Yes | Yes | Yes | No | Yes |
| **5** | High | No | No | Yes | Yes | Yes | No | Yes |
| **6** | High | No | No | Yes | Yes | Yes | No | Yes |
| **7** | High | No | No | No | Yes | Yes | No | No |
| **8** | High | No | No | Yes | Yes | Yes | No | No |
| **9** | High | No | No | Yes | Yes | Yes | No | No |
| **10** | High | Yes | No | Yes | Yes | Yes | No | Yes |
| **11** | High | Yes | No | Yes | Yes | Yes | No | Yes |
| **12** | High | Yes | No | Yes | Yes | Yes | No | Yes |
| **13** | High | No | No | Yes | Yes | Yes | No | Yes |
| **14** | High | No | No | No | Yes | Yes | No | Yes |
| **15** | High | No | No | Yes | Yes | Yes | No | No |
| **16** | High | No | No | No | No | Yes | No | No |
| **17** | High | No | No | No | Yes | Yes | No | Yes |
| **18** | High | No | No | No | No | Yes | No | No |
| **19** | High | No | No | No | Yes | Yes | No | Yes |
| **20** | High | No | No | No | Yes | Yes | No | Yes |
| **21** | High | No | No | Yes | Yes | Yes | No | Yes |

**Table4**.

**Physicochemical properties of potent a-glucosidase inhibitors**

| Comp. | Formula | M.Wt g/mol | Rotable bond | Num.HBA | Num.HBD | i LOGp | WLOGP | TPSA |
|---|---|---|---|---|---|---|---|---|
| **2** | $C_{23}H_{16}N_2O_4$ | 384.38 | 5 | 5 | 2 | 2.94 | 3.93 | 91.90 |
| **3** | $C_{23}H_{16}N_2O_4$ | 384.38 | 5 | 5 | 2 | 2.91 | 3.39 | 90.91 |
| **4** | $C_{23}H_{15}ClN_2O_3$ | 402.83 | 5 | 4 | 1 | 3.5 | 4.88 | 71.67 |
| **5** | $C23H_{15}ClN_2O_3$ | 402.83 | 5 | 4 | 1 | 3.6 | 4.88 | 71.67 |
| **6** | $C_{23}H_{15}ClN_2O_3$ | 402.83 | 5 | 4 | 1 | 3.49 | 4.88 | 71.67 |
| **7** | $C_{23}H_{15}ClN_2O_3$ | 402.83 | 5 | 4 | 1 | 3.49 | 4.88 | 71.67 |
| **8** | $C_{23}H_{15}FN_2O_3$ | 386.38 | 5 | 5 | 1 | 3.36 | 4.78 | 71.67 |
| **9** | $C_{23}H_{15}BrNO_3$ | 447.28 | 5 | 4 | 1 | 3.64 | 4.99 | 71.67 |
| **10** | $C_{23}H_{15}ClN_2O_3$ | 402.83 | 5 | 4 | 1 | 3.5 | 4.88 | 71.67 |
| **11** | $C_{24}H_{18}N_2O_3$ | 382.41 | 5 | 4 | 1 | 3.57 | 4.53 | 71.67 |
| **12** | $C_{24}H_{18}N_2O_3$ | 382.41 | 5 | 4 | 1 | 3.57 | 4.53 | 71.67 |
| **13** | $C_{24}H_{18}N_2O_4$ | 398.41 | 6 | 5 | 1 | 3.48 | 4.23 | 71.67 |
| **14** | $C_{25}H_{20}N_2O_5$ | 428.44 | 7 | 6 | 1 | 3.68 | 4.24 | 71.67 |
| **15** | $C_{27}H_{18}N_2O_3$ | 418.44 | 5 | 4 | 1 | 3.71 | 5.38 | 71.67 |
| **16** | $C_{27}H_{18}N_2O_3$ | 418.44 | 5 | 4 | 1 | 3.71 | 5.38 | 71.67 |
| **17** | $C_{27}H_{18}N_2O_4$ | 434.44 | 5 | 5 | 2 | 3.49 | 5.08 | 91.90 |
| **18** | $C_{23}H_{15}N_3O_5$ | 413.38 | 6 | 6 | 1 | 2.61 | 4.13 | 117.49 |
| **19** | $C_{23}H_{15}N_3O_5$ | 413.38 | 6 | 6 | 1 | 2.81 | 4.13 | 117.49 |
| **20** | $C_{23}H_{15}N_3O_5$ | 413.38 | 6 | 6 | 1 | 2.87 | 4.13 | 117.49 |
| **21** | $C_{21}H_{14}N_2O_4$ | 358.35 | 5 | 5 | 1 | 3.18 | 3.82 | 84.81 |

## Brain or Intestinal Estimate D Permeation

The estimation of two pharmacokinetics behavior is pivotal important, i.e the absorbtion of drug via human gastrointestinal tract and diffusion across the blood brain barriers. In this regards, Brain or Intestinal Estimate D permeation (BOILED-EGG) method was used as an accurate predictive model for computing, to analyze the lipohilicity and polarity behavior of small organic molecules. It is a plot of total polar surface area (TPSA) v/s WLOGP (Daina et al., 2017). The derivatives occurred in the

yellow part (egg yolk region) have higher probability of blood brain barrier permeation, although the derivatives in the white part have high chances of absorption through gastrointestinal tract (GI).

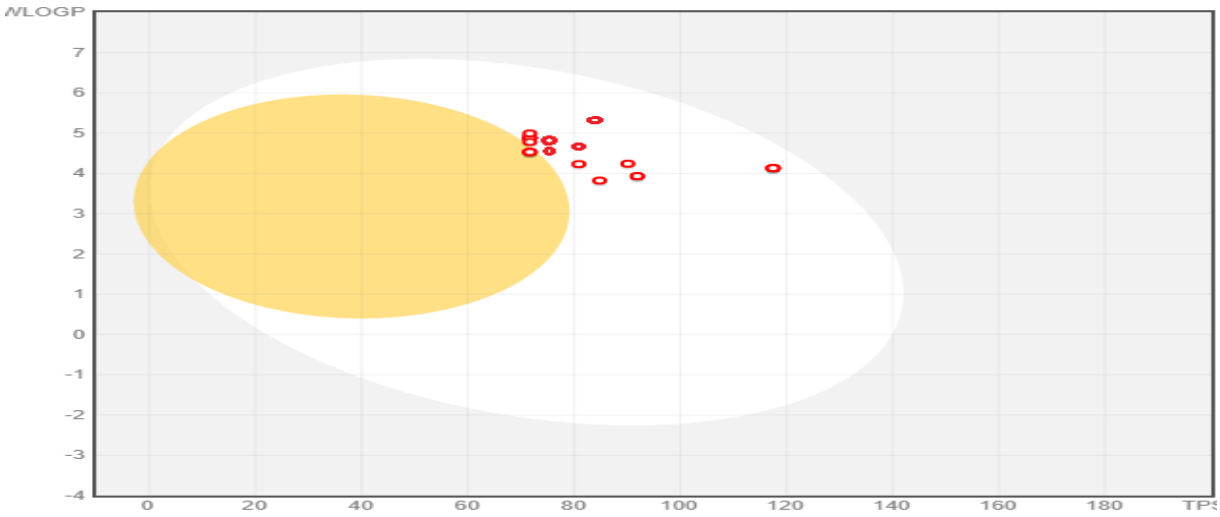


**Figure 10.**
**Showing all the compounds are lying within Egg white region and predicted to be absorbed by Gastrointestinal tract**

### Mapping of Bioavailability Radar of Potent *a*-Glucosidase Inhibitors

Drug-likeness properties LIPOPHILICITY (LIPO), SIZE, POLARITY (POLAR), INSOLUBILITY (INSOLU), INSATURATION (INSATU), FLEXIBILITY (FLEX), was predicted by Drugs mapping bioavailability radar descriptors.

**Table .5 Bioavailability Radar of Potent *a* -Glucosidase Inhibitors**

| Compound | Bioavaibility Radar | LIPO | SIZE | POLAR | INSOLU | INSATU | FLEX |
|---|---|---|---|---|---|---|---|
| **2** | 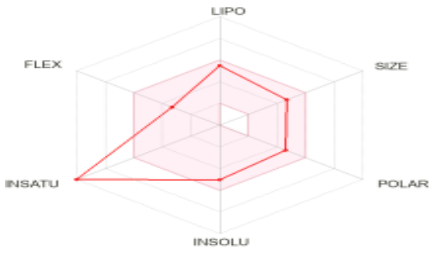 | FPR | FPR | FPR | FPR | SH | FPR |
| **3** | 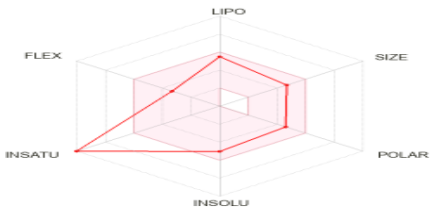 | FPR | FPR | FPR | FPR | SH | FPR |
| **4** | 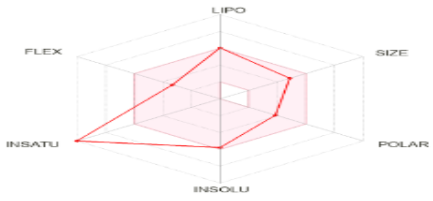 | FPR | FPR | FPR | FPR | SH | FPR |

| | | | | | | | |
|---|---|---|---|---|---|---|---|
| 5 | 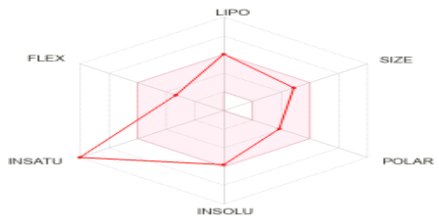 | FPR | FPR | FPR | FPR | SH | FPR |
| 6 | 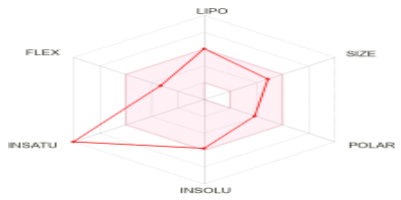 | FPR | FPR | FPR | FPR | SH | FPR |
| 7 | 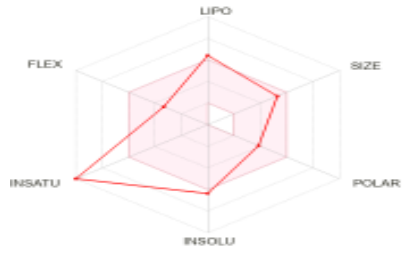 | FPR | FPR | FPR | FPR | SH | FPR |
| 8 |  | FPR | FPR | FPR | FPR | SH | FPR |
| 9 | 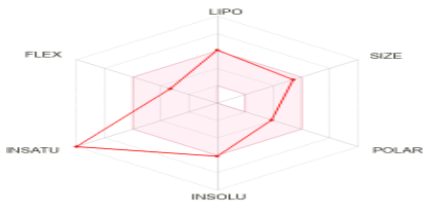 | FPR | FPR | FPR | FPR | SH | FPR |
| 10 | 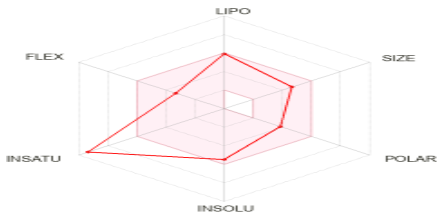 | FPR | FPR | FPR | FPR | SH | FPR |
| 11 | 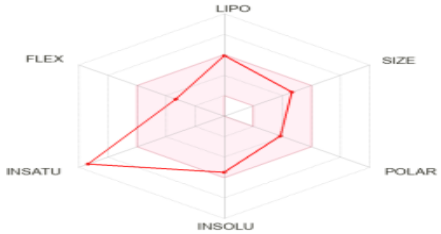 | FPR | FPR | FPR | FPR | SH | FPR |

| | | | | | | | |
|---|---|---|---|---|---|---|---|
| **12** | 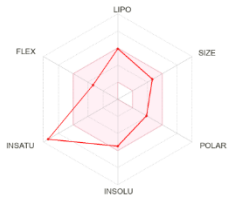 | FPR | FPR | FPR | FPR | SH | FPR |
| **13** | 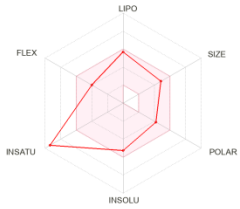 | FPR | FPR | FPR | FPR | SH | FPR |
| **14** | 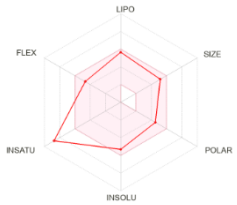 | FPR | FPR | FPR | FPR | SH | FPR |
| **15** | 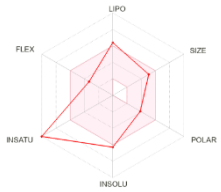 | FPR | FPR | FPR | FPR | SH | FPR |
| **16** | 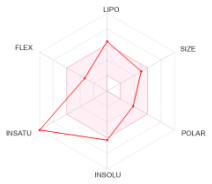 | FPR | FPR | FPR | FPR | SH | FPR |

| | | | | | | | |
|---|---|---|---|---|---|---|---|
| **17** | 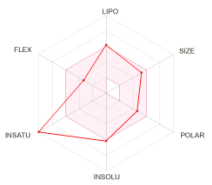 | FPR | FPR | FPR | FPR | SH | FPR |
| **18** | 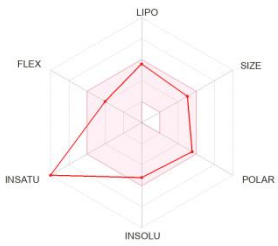 | FPR | FPR | FPR | FPR | SH | FPR |

| | | | | | | | |
|---|---|---|---|---|---|---|---|
| **19** | 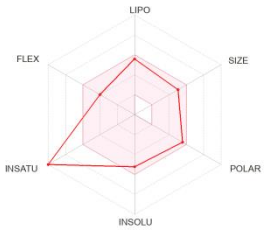 | FPR | FPR | FPR | FPR | SH | FPR |
| **20** | 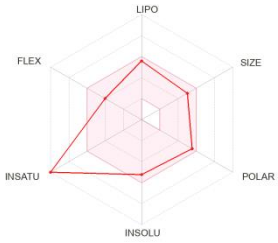 | FPR | FPR | FPR | FPR | SH | FPR |
| **21** | 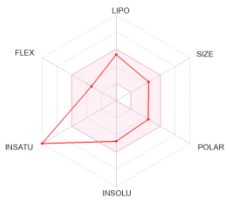 | FPR | FPR | FPR | FPR | SH | FPR |

*FPR= Flavourable with in the pink region,
*SH=Slightly high

## H$^1$NMR C$^{13}$ NMR and ESI MS and Elemental (CHN/S) Analysis

At present we have received only ESI MS from our collaborator although we have also performed Elemental (CHN/S). On the basis of these results we have performed enzyme inhibition and molecular docking studies.

## N-2-hydroxy phenyl-2-[4-(4-oxo-3,4-dihydro-2H-1-benzopyran-2-yl) benzoyl] hydrazine -1-carbothioamide 2

Solid; Yield: 81%; M.P. 324°C; 1HNMR (300MHz, DMSO-d6): 5.0(s,J=5Hz,1H-OH), 6.29(d, J=7.26Hz,2H) 6.48(d, 7.26Hz, 2H), 7.9 (d, J=7.26Hz, 2H) 7.48(d, J=7.26Hz,2H), 6.75(s,J=7.26Hz,1H), 6.84(s, J=7.26Hz,1H), 7.11(s, J=7.26Hz,1H),8.0(s, J=8.0Hz, 1H,N-NH), 4.0(s,J=4.0Hz, 1H,N-C)$^{13}$CNMR (150MHz, DMSO-$d_6$; Anal. Calcd for $C_{23}H_{17}N_3O_5S$, C = 61.74, H = 3.83, N = 9.39, S = 7.17; Found C = 61.62, H = 3.78, N = 9.34, S = 7.12; ESI MS *m/z* (% rel. abund.): 447.44$[M+1]^+$.

## N-4-hydroxy phenyl-2-[4-(4-oxo-3,4-dihydro-2H-1-benzopyran-2-yl) benzoyl] hydrazine -1-carbothioamide 3

Solid; Yield: 87%; M.P. 311°C; $^1$HNMR (300MHz, DMSO-$d_6$): 6.84(s, J=7.26Hz, 1H), 7.11(s, J=7.26Hz,1H),6.75(s, J=7.26Hz,1H), 7.48(s,J=7.26Hz,2H) 7.90(d, J=7.26Hz,2H), 8.0(s, J=8.0Hz,1H sec amide) 2.0(s,J=2.0Hz,1H amine), 4.0(s, J=4.0Hz, 1H C-NH) 6.48(s, J=7.26Hz,1H), 6.45( s,J=7.26Hz,1H) 6.57(s, J=7.26Hz,1H) 6.29(s,J=7.26Hz,1H)

5.0(d,J=5.0,2H), 6.71(s,J=5.25Hz,1H)$^{13}$CNMR (150MHz, DMSO-$d_6$; Anal. Calcd for $C_{23}H_{17}N_3O_5S$, C = 61.74, H = 3.83, N = 9.39, S = 7.17; Found C = 61.63, H = 3.73, N = 9.32, S = 7.10; ESI MS *m/z* (% rel. abund.): 447.23$[M+1]^+$.

## N-2-chloro phenyl-2-[4-(4-oxo-3,4-dihydro-2H-1-benzopyran-2-yl) benzoyl] hydrazine -1-carbothioamide 4

Solid; Yield: 87%; M.P. 288°C; $^{1}$HNMR (300MHz, DMSO-$d_6$): 6.84(s, J=7.26Hz,1H), 7.11(s,J=7.26Hz,1H)6.75(s, J=7.26Hz,1H), 7.48(d,J=7.26Hz,2H)7.90(d,J=7.26Hz,2H), 5.0(s, J=5.0Hz,1H)8.0(s,J=8.0Hz,1Hsec amide), 2.0(s,J=2.0Hz amine)4.0(s,J=4.0Hz C-NH) 7.02(s,J=7.26Hz) 6.56(s,J=7.26 1Hz)6.89(s, J=7.26Hz,1H) 6.40(s,J=7.26Hz,1H) $^{13}$CNMR (150MHz, DMSO-$d_6$; Anal. Calcd for $C_{23}H_{16}ClN_3O_4S$, C = 59.29, H = 3.46, N = 9.02, S = 6.88; Found C = 59.24, H = 3.40, N = 9.00, S = 6.81; ESI MS *m/z* (% rel. abund.): 465.31$[M+1]^+$, 467.15 $[M+2]^+$.

## N-3-chloro phenyl-2-[4-(4-oxo-3,4-dihydro-2H-1-benzopyran-2-yl) benzoyl] hydrazine -1-carbothioamide 5

Solid; Yield: 87%; M.P. 296°C; $^{1}$HNMR (300MHz, DMSO-$d_6$): 6.84(s, J=7.26Hz,1H), 7.11(s,J=7.26Hz,1H), 6.75(s, J=7.26Hz,1H), 7.48(d,J=7.26Hz,2H), 7.90(d,J=7.26Hz,2H), 5.0(s, J=5.0Hz,1H), 8.0(s,J=8.0Hz,1Hsec amide), 2.0(s,J=2.0Hz amine), 4.0(s,J=4.0Hz C-NH),6.47(s,J=7.26Hz,1H),6.63(s,J=7.26,1Hz),6.95(s,J=7.26Hz,1H),6.34(s,J=7.26Hz,1H), 6.71(s,J=7.26Hz,1H).$^{13}$CNMR (150MHz, DMSO-$d_6$; Anal. Calcd for $C_{23}H_{16}ClN_3O_4S$, C = 59.29, H = 3.46, N = 9.02, S = 6.88; Found C = 59.26, H = 3.42, N = 9.01, S = 6.83; ESI MS *m/z* (% rel. abund.): 465.22$[M+1]^+$, 467.11 $[M+2]^+$.

## N-4-chloro phenyl-2-[4-(4-oxo-3,4-dihydro-2H-1-benzopyran-2-yl) benzoyl] hydrazine -1-carbothioamide 6

Solid; Yield: 81%; M.P. 304°C; $^{1}$HNMR (300MHz, DMSO-$d_6$): 6.84(s, J=7.26Hz,1H), 7.11(s,J=7.26Hz,1H), 6.75(s, J=7.26Hz,1H), 7.48(d,J=7.26Hz,2H), 7.90(d,J=7.26Hz,2H), 5.0(s, J=5.0Hz,1H), 8.0(s,J=8.0Hz,1Hsec amide), 2.0(s,J=2.0Hz amine), 4.0(s,J=4.0Hz C-NH), 6.40(d,J=7.26Hz,2H), 7.02(d,J=7.26,2Hz), 6.40(s,J=7.26Hz,1H), 6.71 (s,J=7.26Hz ,1H).$^{13}$CNMR (150MHz, DMSO-$d_6$; Anal. Calcd for $C_{23}H_{16}ClN_3O_4S$, C = 59.29, H = 3.46, N = 9.02, S = 6.88; Found C = 59.20, H = 3.41, N = 9.00, S = 6.83; ESI MS *m/z* (% rel. abund.): 465.16$[M+1]^+$, 467.23 $[M+2]^+$.

## N-2,4-dichlorophenyl-2-[4-(4-oxo-3,4-dihydro-2H-1-benzopyran-2-yl) benzoyl] hydrazine -1-carbothioamide 7

Solid; Yield: 83%; M.P. 322°C; $^{1}$HNMR (300MHz, DMSO-$d_6$): 6.84(s, J=7.26Hz,1H), 7.11(s,J=7.26Hz,1H), 6.75(s, J=7.26Hz,1H), 7.48(d,J=7.26Hz,2H), 7.90(d,J=7.26Hz,2H), 5.0(s, J=5.0Hz,1H), 8.0(s,J=8.0Hz,1Hsec amide), 2.0(s,J=2.0Hz amine), 4.0(s,J=4.0Hz C-NH), 7.03(s,J=7.26Hz,1H), 6.90(s,J=7.26Hz,1H), 6.34(s, J=7.26Hz,1H), 6.71 (s,J=5.25 Hz,1H), $^{13}$CNMR (150MHz, DMSO-$d_6$; Anal. Calcd for $C_{23}H_{15}Cl_2N_3O_4S$, C = 55.21, H= 3.02, N = 8.40, S = 6.41; Found C = 55.17, H = 3.01, N = 8.36, S = 6.38; ESI MS *m/z* (% rel. abund.): 499.13$[M+1]^+$, 501.31$[M+2]^+$, 503.14$[M+4]^+$.

## N-4-florophenyl-2-[4-(4-oxo-3,4-dihydro-2H-1-benzopyran-2-yl) benzoyl] hydrazine -1-carbothioamide 8

Solid; Yield: 82%; M.P. 314°C; $^{1}$HNMR (300MHz, DMSO-$d_6$): 6.84(s, J=7.26Hz,1H), 7.11(s,J=7.26Hz,1H), 6.75(s, J=7.26Hz,1H), 7.48(d,J=7.26Hz,2H), 7.90(d,J=7.26Hz,2H), 5.0(s, J=5.0Hz,1H), 8.0(s,J=8.0Hz,1Hsec amide), 2.0(s,J=2.0Hz amine), 4.0(s,J=4.0Hz C-NH),6.44(d,J=7.26Hz,2H), 6.72(d,J=7.26 Hz,2H), 6.71(s, J=5.25Hz,1H).

$^{13}$CNMR (150MHz, DMSO-$d_6$; Anal. Calcd for $C_{23}H_{16}FN_3O_4S$, C = 61.46, H = 3.59, N = 9.35, S = 7.13; Found C = 61.40, H = 3.53, N = 9.33, S = 7.10; ESI MS *m/z* (% rel. abund.): 449.24$[M+1]^+$, 451.21$[M+2]^+$.

### N-4-bromo phenyl-2-[4-(4-oxo-3,4-dihydro-2H-1-benzopyran-2-yl) benzoyl] hydrazine -1-carbothioamide 9

Solid; Yield: 74%; M.P. 322°C; $^1$HNMR (300MHz, DMSO-$d_6$): 6.84(s, J=7.26Hz,1H), 7.11(s,J=7.26Hz,1H), 6.75(s, J=7.26Hz,1H), 7.48(d,J=7.26Hz,2H),7.90(d,J=7.26Hz,2H), 5.0(s, J=5.0Hz,1H), 8.0(s,J=8.0Hz,1Hsec amide), 2.0(s,J=2.0Hz amine), 4.0(s,J=4.0Hz C-NH), 6.35(d,J=7.26Hz,2H), 7.18(d,J=7.26 Hz,2H), 6.71(s, J=5.25Hz,1H). $^{13}$CNMR (150MHz, DMSO-$d_6$; Anal. Calcd for $C_{23}H_{16}BrN_3O_4S$, C = 54.13, H = 3.16, N = 8.23, S = 6.28; Found C = 54.08, H = 3.13, N = 8.22, S = 6.22; ESI MS *m/z* (% rel. abund.): 509.44$[M+1]^+$, 511.22$[M+2]^+$.

### N-2-methyl phenyl-2-[4-(4-oxo-3,4-dihydro-2H-1-benzopyran-2-yl) benzoyl] hydrazine -1-carbothioamide 10

Solid; Yield: 84%; M.P. 280°C; $^1$HNMR (300MHz, DMSO-$d_6$): 6.84(s, J=7.26Hz,1H), 7.11(s,J=7.26Hz,1H), 6.75(s, J=7.26Hz,1H), 7.48(d,J=7.26Hz,2H), 7.90(d,J=7.26Hz,2H), 5.0(s, J=5.0Hz,1H), 8.0(s,J=8.0Hz,1Hsec amide), 2.0(s,J=2.0Hz amine), 4.0(s,J=4.0Hz C-NH), 6.81(s,J=7.26Hz,1H), 6.50(s,J=7.26 Hz,1H), 6.82(s, J=7.26Hz,1H), 6.34(s, J=7.26Hz,1H), 2.35(m, J=0.86Hz,3H), 6.71(s,J=5.25 Hz,1H). $^{13}$CNMR (150MHz, DMSO-$d_6$; Anal. Calcd for $C_{24}H_{19}N_3O_4S$, C = 64.71, H = 4.30, N = 9.43, S = 7.20; Found C = 64.65, H = 4.28, N = 9.38, S = 7.17; ESI MS *m/z* (% rel. abund.): 445.37$[M+1]^+$.

### N-3-methyl phenyl-2-[4-(4-oxo-3,4-dihydro-2H-1-benzopyran-2-yl) benzoyl] hydrazine -1-carbothioamide 11

Solid; Yield: 87%; M.P. 274°C; $^1$HNMR (300MHz, DMSO-$d_6$): 6.84(s, J=7.26Hz,1H), 7.11(s,J=7.26Hz,1H), 6.75(s, J=7.26Hz,1H), 7.48(d,J=7.26Hz,2H), 7.90(d,J=7.26Hz,2H), 5.0(s, J=5.0Hz,1H), 8.0(s,J=8.0Hz,1Hsec amide), 2.0(s,J=2.0Hz amine), 4.0(s,J=4.0Hz C-NH), 6.26(s,J=7.26Hz,1H), 6.42(s,J=7.26 Hz,1H), 6.89(s, J=7.26Hz,1H), 6.27(s, J=7.26Hz,1H), 2.35(m, J=0.86Hz,3H), 6.71(s,J=5.25 Hz,1H). $^{13}$CNMR (150MHz, DMSO-$d_6$; Anal. Calcd for $C_{24}H_{19}N_3O_4S$, C = 64.71, H = 4.30, N = 9.43, S = 7.20; Found C = 64.66, H = 4.27, N = 9.31, S = 7.18; ESI MS *m/z* (% rel. abund.): 445.55$[M+1]^+$.

### N-4-methyl phenyl-2-[4-(4-oxo-3,4-dihydro-2H-1-benzopyran-2-yl) benzoyl] hydrazine -1-carbothioamide 12

Solid; Yield: 83%; M.P. 281°C; $^1$HNMR (300MHz, DMSO-$d_6$): 6.84(s, J=7.26Hz,1H), 7.11(s,J=7.26Hz,1H), 6.75(s, J=7.26Hz,1H), 7.48(d,J=7.26Hz,2H), 7.90(d,J=7.26Hz,2H), 5.0(s, J=5.0Hz,1H), 8.0(s,J=8.0Hz,1Hsec amide), 2.0(s,J=2.0Hz amine), 4.0(s,J=4.0Hz C-NH), 6.34(d,J=7.26Hz,2H), 6.81(d,J=7.26 Hz,2H), 2.35(m, J=0.86Hz,3H) 6.71(s,J=5.25 Hz,1H)$^{13}$CNMR (150MHz, DMSO-$d_6$; Anal. Calcd for $C_{24}H_{19}N_3O_4S$, C = 64.71, H = 4.30, N = 9.43, S = 7.20; Found C = 64.68, H = 4.26, N = 9.37, S = 7.17; ESI MS *m/z* (% rel. abund.): 445.46$[M+1]^+$.

### N-2-methoxy phenyl-2-[4-(4-oxo-3,4-dihydro-2H-1-benzopyran-2-yl) benzoyl] hydrazine -1-carbothioamide 13

Solid; Yield: 92%; M.P. 304°C; $^1$HNMR (300MHz, DMSO-$d_6$): 6.84(s, J=7.26Hz,1H), 7.11(s,J=7.26Hz,1H), 6.75(s, J=7.26Hz,1H), 7.48(d,J=7.26Hz,2H), 7.90(d,J=7.26Hz,2H), 5.0(s, J=5.0Hz,1H), 8.0(s,J=8.0Hz,1Hsec amide), 2.0(s,J=2.0Hz amine), 4.0(s,J=4.0Hz C-

NH), 6.35(d,J=7.26Hz,2H), 6.52(d,J=7.26 Hz,2H), 3.73(m, J=0.86Hz,3H) 6.71(s,J=5.25 Hz,1H) $^{13}$CNMR (150MHz, DMSO-$d_6$; Anal. Calcd for $C_{24}H_{19}N_3O_5S$, C = 62.46, H = 4.15, N = 9.11, S = 6.95; Found C = 64.43, H = 4.11, N = 9.05, S = 6.88; ESI MS *m/z* (% rel. abund.): 461.17[M+1]$^+$.

## N-2,5-dimethoxy phenyl-2-[4-(4-oxo-3,4-dihydro-2H-1-benzopyran-2-yl) benzoyl] hydrazine -1-carbothioamide 14

Solid; Yield: 88%; M.P. 282°C; $^1$HNMR (300MHz, DMSO-$d_6$): 6.84(s, J=7.26Hz,1H), 7.11(s,J=7.26Hz,1H), 6.75(s, J=7.26Hz,1H), 7.48(d,J=7.26Hz,2H), 7.90(d,J=7.26Hz,2H), 5.0(s, J=5.0Hz,1H), 8.0(s,J=8.0Hz,1Hsec amide), 2.0(s,J=2.0Hz amine), 4.0(s,J=4.0Hz C-NH), 6.03(s,J=7.26Hz,1H), 6.08(s,J=7.26 Hz,1H), 6.24(s,J=7.26 Hz,1H) 3.73(m, J=0.86Hz,6H) 6.71(s,J=5.25 Hz,1H) $^{13}$CNMR (150MHz, DMSO-$d_6$; Anal. Calcd for $C_{25}H_{21}N_3O_6S$, C = 61.09, H = 4.31, N = 8.55, S = 6.52; Found C = 61.03, H = 4.27, N = 8.51, S = 6.48; ESI MS *m/z* (% rel. abund.): 491.21[M+1]$^+$.

## N-1-napthyl -2-[4-(4-oxo-3,4-dihydro-2H-1-benzopyran-2-yl) benzoyl] hydrazine -1-carbothioamide 15

Solid; Yield: 83%; M.P. =276°C; $^1$HNMR (300MHz, DMSO-$d_6$): 6.84(s, J=7.26Hz,1H), 7.11(s,J=7.26Hz,1H), 6.75(s, J=7.26Hz,1H), 7.48(d,J=7.26Hz,2H), 7.90(d,J=7.26Hz,2H), 5.0(s, J=5.0Hz,1H), 8.0(s,J=8.0Hz,1Hsec amide), 2.0(s,J=2.0Hz amine), 4.0(s,J=4.0Hz C-NH), 6.76(s,J=7.32Hz,1H), 7.51(s,J=7.67 Hz,1H), 6.79(s,J=7.67 Hz,1H) 7.55(s,J=7.67 Hz,1H) 7.09(s,J=7.32 Hz,1H) 7.23(s,J=7.32 Hz,1H) 7.44(s,J=7.67 Hz,1H) 6.71(s,J=5.25 Hz,1H)$^{13}$CNMR (150MHz, DMSO-$d_6$; Anal. Calcd for $C_{27}H_{19}N_3O_4S$, C = 67.35, H = 3.98, N = 8.37, S = 6.66; Found C = 67.29, H = 3.91, N = 8.33, S = 6.62; ESI MS *m/z* (% rel. abund.): 481.13[M+1]$^+$.

## N-2- napthyl -2-[4-(4-oxo-3,4-dihydro-2H-1-benzopyran-2-yl) benzoyl] hydrazine -1-carbothioamide 16

Solid; Yield: 81%; M.P. 282°C; $^1$HNMR (300MHz, DMSO-$d_6$): 6.84(s, J=7.26Hz,1H), 7.11(s,J=7.26Hz,1H), 6.75(s, J=7.26Hz,1H), 7.48(d,J=7.26Hz,2H), 7.90(d,J=7.26Hz,2H), 5.0(s, J=5.0Hz,1H), 8.0(s,J=8.0Hz,1Hsec amide), 2.0(s,J=2.0Hz amine), 4.0(s,J=4.0Hz C-NH), 6.76(s,J=7.32Hz,1H), 7.51(s,J=7.67 Hz,1H), 6.79(s,J=7.67 Hz,1H) 7.55(s,J=7.67 Hz,1H) 7.09(s,J=7.32 Hz,1H) 7.23(s,J=7.32 Hz,1H) 7.44(s,J=7.67 Hz,1H) 6.71(s,J=5.25 Hz,1H) $^{13}$CNMR (150MHz, DMSO-$d_6$; Anal. Calcd for $C_{27}H_{19}N_3O_4S$, C = 67.35, H = 3.98, N = 8.37, S = 6.66; Found C = 67.31, H = 3.90, N = 8.33, S = 6.63; ESI MS *m/z* (% rel. abund.): 481.13[M+1]$^+$.

## N-2-hydroxynapthyl-2-[4-(4-oxo-3,4-dihydro-2H-1-benzopyran-2-yl) benzoyl] hydrazine -1-carbothioamide 17

Solid; Yield: 87%; M.P. 315°C; $^1$HNMR (300MHz, DMSO-$d_6$): 6.84(s, J=7.26Hz,1H), 7.11(s,J=7.26Hz,1H), 6.75(s, J=7.26Hz,1H), 7.48(d,J=7.26Hz,2H), 7.90(d,J=7.26Hz,2H), 5.0(s, J=5.0Hz,1H), 8.0(s,J=8.0Hz,1Hsec amide), 2.0(s,J=2.0Hz amine), 4.0(s,J=4.0Hz C-NH), 6.82(s,J=7.67Hz,1H), 6.74(s,J=7.67 Hz,1H), 7.41(s,J=7.67 Hz,1H) 7.07(s,J=7.32 Hz,1H) 7.12(s,J=7.32 Hz,1H) 7.40(s,J=7.67 Hz,1H) 5.0(s,J=5.25 Hz,1HO) 6.71(s,J=5.25 Hz,1H) $^{13}$CNMR (150MHz, DMSO-$d_6$; Anal. Calcd for $C_{27}H_{19}N_3O_5S$, C = 65.18, H = 3.85, N = 8.45, S = 6.44; Found C = 65.10, H = 3.82, N = 8.41, S = 6.40; ESI MS *m/z* (% rel. abund.): 497.18[M+1]$^+$.

## N-2-nitrophenyl-2-[4-(4-oxo-3,4-dihydro-2H-1-benzopyran-2-yl) benzoyl] hydrazine -1-carbothioamide 18

Solid; Yield: 78%; M.P. 313°C; $^{1}$HNMR (300MHz, DMSO-$d_6$): 6.84(s, J=7.26Hz,1H), 7.11(s,J=7.26Hz,1H), 6.75(s, J=7.26Hz,1H), 7.48(d,J=7.26Hz,2H), 7.90(d,J=7.26Hz,2H), 5.0(s, J=5.0Hz,1H), 8.0(s,J=8.0Hz,1Hsec amide), 2.0(s,J=2.0Hz amine), 4.0(s,J=4.0Hz C-NH), 7.94(s,J=7.26Hz,1H), 6.88(s,J=7.26 Hz,1H), 7.40(s,J=7.26 Hz,1H) 6.72(s,J=7.26 Hz,1H) 6.71(s,J=5.25 Hz,1H) $^{13}$CNMR (150MHz, DMSO-$d_6$; Anal. Calcd for $C_{23}H_{16}N_4O_6S$, C = 57.98, H = 3.38, N = 11.76, S = 6.73; Found C = 57.91, H = 3.34, N = 11.70, S = 6.71; ESI MS *m/z* (% rel. abund.): 476.16$[M+1]^+$.

### N-3-nitrophenyl-2-[4-(4-oxo-3,4-dihydro-2H-1-benzopyran-2-yl) benzoyl] hydrazine -1-carbothioamide 19

Solid; Yield: 85%; M.P. 321°C; $^{1}$HNMR (300MHz, DMSO-$d_6$): 6.84(s, J=7.26Hz,1H), 7.11(s,J=7.26Hz,1H), 6.75(s, J=7.26Hz,1H), 7.48(d,J=7.26Hz,2H), 7.90(d,J=7.26Hz,2H), 5.0(s, J=5.0Hz,1H), 8.0(s,J=8.0Hz,1Hsec amide), 2.0(s,J=2.0Hz amine), 4.0(s,J=4.0Hz C-NH), 7.39(s,J=7.26Hz,1H), 7.55(s,J=7.26 Hz,1H), 7.27(s,J=7.26 Hz,1H) 6.85(s,J=7.26 Hz,1H) 6.71(s,J=5.25 Hz,1H) $^{13}$CNMR (150MHz, DMSO-$d_6$; Anal. Calcd for $C_{22}H_{16}N_2O_5$, $C_{23}H_{16}N_4O_6S$, C = 57.98, H = 3.38, N = 11.76, S = 6.73; Found C = 57.93, H = 3.34, N = 11.69, S = 6.73; ESI MS *m/z* (% rel. abund.): 476.22$[M+1]^+$.

### N-4-nitro phenyl-2-[4-(4-oxo-3,4-dihydro-2H-1-benzopyran-2-yl) benzoyl] hydrazine -1-carbothioamide 20

Solid; Yield: 85%; M.P. 328°C; $^{1}$HNMR (300MHz, DMSO-$d_6$): 6.84(s, J=7.26Hz,1H), 7.11(s,J=7.26Hz,1H), 6.75(s, J=7.26Hz,1H), 7.48(d,J=7.26Hz,2H), 7.90(d,J=7.26Hz,2H), 5.0(s, J=5.0Hz,1H), 8.0(s,J=8.0Hz,1Hsec amide), 2.0(s,J=2.0Hz amine), 4.0(s,J=4.0Hz C-NH), 6.72(d,J=7.26Hz,2H), 7.94(d,J=7.26 Hz,2H), 6.71(s,J=5.25 Hz,1H) $^{13}$CNMR (150MHz, DMSO-$d_6$; Anal. Calcd for $C_{23}H_{16}N_4O_6S$, C = 57.98, H = 3.38, N = 11.76, S = 6.73; Found C = 57.90, H = 3.30, N = 11.71, S = 6.69; ESI MS m/z (% rel. abund.): 476.14$[M+1]^+$.

### N-furfuryl-2-[4-(4-oxo-3,4-dihydro-2H-1-benzopyran-2-yl) benzoyl] hydrazine -1-carbothioamide 21

Solid; Yield: 81%; M.P. 274°C; $^{1}$HNMR (300MHz, DMSO-$d_6$): 6.84(s, J=7.26Hz,1H), 7.11(s,J=7.26Hz,1H), 6.75(s, J=7.26Hz,1H), 7.48(d,J=7.26Hz,2H), 7.90(d,J=7.26Hz,2H), 5.0(s, J=5.0Hz,1H), 8.0(s,J=8.0Hz,1Hsec amide), 2.0(s,J=2.0Hz amine), 4.0(s,J=4.0Hz C-NH), 6.3(d,J=6.3Hz,2H), 7.4(s,J=7.38 Hz,1H), 6.71(s,J=5.25 Hz,1H) $^{13}$CNMR (150MHz, DMSO-$d_6$; Anal. Calcd for $C_{21}H_{15}N_3O_5S$, C = 59.85, H = 3.59, N = 9.97, S = 7.61; Found C = 59.81, H = 3.54, N = 9.93, S = 7.54; ESI MS *m/z* (% rel. abund.): 421.16$[M+1]^+$.

## DECLARATIONS

**Acknowledgement:** We appreciate the generous support from all the contributor to the research and their different affiliations.

**Funding:** No funding body in the public, private, or nonprofit sectors provided a particular grant for this research.

**Availability of data and material:** In the approach, the data sources for the variables are stated.

**Authors' contributions:** Each author participated equally in the creation of this work.

**Conflicts of Interest:** The authors declare no conflict of interest.

**Consent to Participate:** Yes

**Consent for publication and Ethical approval:** Because this study does not include human or animal data, ethical approval is not required for publication. All authors have given their consent.

# REFERENCES


Akkati, S., Sam, K. G., & Tungha, G. (2011). Emergence of promising therapies in diabetes mellitus. *Journal of Clinical Pharmacology*, *51*(6), 796–804. https://doi.org/10.1177/0091270010376972

Chen, L., Magliano, D. J., & Zimmet, P. Z. (2012). The worldwide epidemiology of type 2 diabetes mellitus - Present and future perspectives. In *Nature Reviews Endocrinology* (Vol. 8, Issue 4, pp. 228–236). https://doi.org/10.1038/nrendo.2011.183

Choi, Y. J., & Chung, Y.-S. (2016). Type 2 diabetes mellitus and bone fragility: Special focus on bone imaging. *Osteoporosis and Sarcopenia*, *2*(1), 20–24. https://doi.org/10.1016/j.afos.2016.02.001

Craig, M. E., Hattersley, A., & Donaghue, K. C. (2009). Definition, epidemiology and classification of diabetes in children and adolescents. *Pediatric Diabetes*, *10*(SUPPL. 12), 3–12. https://doi.org/10.1111/j.1399-5448.2009.00568.x

Daina, A., Michielin, O., & Zoete, V. (2017). SwissADME: A free web tool to evaluate pharmacokinetics, drug-likeness and medicinal chemistry friendliness of small molecules. *Scientific Reports*, *7*. https://doi.org/10.1038/srep42717

Daina, A., & Zoete, V. (2016). A BOILED-Egg To Predict Gastrointestinal Absorption and Brain Penetration of Small Molecules. *ChemMedChem*, 1117–1121. https://doi.org/10.1002/cmdc.201600182

Daneman, D. (2006). Type 1 diabetes. In *www.thelancet.com* (Vol. 367). www.thelancet.com

Devendra, D., Liu, E., & Eisenbarth, G. S. (n.d.). *Clinical review Type 1 diabetes: recent developments*. www.barbaradaviscenter.org

Maahs, D. M., West, N. A., Lawrence, J. M., & Mayer-Davis, E. J. (2010). Epidemiology of type 1 diabetes. In *Endocrinology and Metabolism Clinics of North America* (Vol. 39, Issue 3, pp. 481–497). W.B. Saunders. https://doi.org/10.1016/j.ecl.2010.05.011

Malek, R., Hannat, S., Nechadi, A., Mekideche, F. Z., & Kaabeche, M. (2019). Diabetes and Ramadan: A multicenter study in Algerian population. In *Diabetes Research and Clinical Practice* (Vol. 150, pp. 322–330). Elsevier Ireland Ltd. https://doi.org/10.1016/j.diabres.2019.02.008

Picke, A. K., Campbell, G., Napoli, N., Hofbauer, L. C., & Rauner, M. (2019). Update on the impact of type 2 diabetes mellitus on bone metabolism and material properties. In *Endocrine Connections* (Vol. 8, Issue 3, pp. R55–R70). BioScientifica Ltd. https://doi.org/10.1530/EC-18-0456

Proença, C., Freitas, M., Ribeiro, D., Oliveira, E. F. T., Sousa, J. L. C., Tomé, S. M., Ramos, M. J., Silva, A. M. S., Fernandes, P. A., & Fernandes, E. (2017). α-Glucosidase inhibition by flavonoids: an in vitro and in silico structure–activity relationship study. *Journal of Enzyme Inhibition and Medicinal Chemistry*, *32*(1), 1216–1228. https://doi.org/10.1080/14756366.2017.1368503

World Health Organization, & International Diabetes Federation. (n.d.). *Definition and diagnosis of diabetes mellitus and intermediate hyperglycaemia : report of a WHO/IDF consultation*.

Yousuf, M., Mammadova, K., Khan, L., Professor, A., Karachi, S., & Author, C. (2018). Bioinformatics Review Homology Modeling of α-Glucosidase Enzyme: 3D Structure Prediction. *Bioinformatics Review*, *4*(11), 9–14. www.bioinformaticsreview.com

Zheng, Y., Ley, S. H., & Hu, F. B. (2018). Global aetiology and epidemiology of type 2 diabetes mellitus and its complications. In *Nature Reviews Endocrinology* (Vol. 14, Issue 2, pp. 88–98). Nature Publishing Group. https://doi.org/10.1038/nrendo.2017.151